Charge transport in cobalt-doped iron pyrite

S. Guo,[1] D. P. Young,[1] R. T. Macaluso,[2] D. A. Browne,[1] N. L. Henderson,[1] J. Y. Chan,[2] L. L. Henry,[3] and J. F. DiTusa[1]
[1]*Department of Physics and Astronomy, Louisiana State University, Baton Rouge, Louisiana 70803, USA*
[2]*Department of Chemistry, Louisiana State University, Baton Rouge, Louisiana 70803, USA*
[3]*Department of Physics, Southern University, Baton Rouge, Louisiana 70813 USA*
(Received 14 December 2009; revised manuscript received 11 March 2010; published 26 April 2010)

The Hall effect and resistivity of the carrier-doped magnetic semiconductor $Fe_{1-x}Co_xS_2$ were measured for $0 \leq x \leq 0.16$, temperatures between 0.05 and 300 K, and fields of up to 9 T. Our Hall data indicate electron charge carriers with a density of only 10–30 % of the Co density of our crystals. The charge-carrier transport is dominated by a Kondo-like anomaly below 20 K for x less than that required to form a long-range magnetic state, x_c. For $x > x_c$, the resistivity and magnetoresistance resemble that of a spin glass with a reduction in the resistivity by as much as 35% in 5 T fields. Although the product of the Fermi wave vector and the mean-free path, $k_F\ell$, varies between 1.5 and 15 over the range of x investigated, we observe no indication of quantum corrections to the resistivity, ρ, as ρ is dominated by the Kondo and spin glasslike anomalies down to very low temperature. Despite the previous identification of magnetic Griffiths phase formation in the magnetic and thermodynamic properties of this system for the same range of x, we measure a saturating resistivity below 0.5 K indicating Fermi liquidlike transport. We also observe an enhancement of the residual resistivity ratio by almost a factor of 2 for samples with $x \sim x_c$ indicating temperature-dependent scattering mechanisms beyond simple carrier-phonon scattering. We speculate that this enhancement is due to charge carrier scattering from magnetic fluctuations which contribute to the resistivity over a wide temperature range.

DOI: 10.1103/PhysRevB.81.144424 PACS number(s): 71.30.+h, 72.15.Gd, 72.15.Qm, 72.15.Rn

I. INTRODUCTION AND MOTIVATION

Magnetic semiconductors have been of great recent interest because of their promise as sources of polarized currents for spintronics applications.[1,2] Typically transition-metal atoms are substituted into paramagnetic insulators to create semiconducting or metallic ferromagnetic phases.[3–6] The substitution level required to nucleate ferromagnetism is usually a few percent so that the doping-induced disorder can be significant while carrier densities remain well below that of prototypical metals. These systems are clearly distinct from the well-studied paramagnetic semiconductors and the metallic or insulating magnets because they exhibit a combination of metal-insulator transition physics with the emergence of magnetism. The charge transport is characterized by short mean-free paths, ℓ, and associated high resistivities, however the low-temperature, T, transport properties can reveal behavior quite different from that of simple semiconducting systems.[7–11] Recent discoveries include enormous anomalous Hall effects and non-Fermi-liquid (NFL) transport.[3,12–15]

At the same time, there has been enormous interest[16–22] over the past decade in systems that can be tuned via pressure, magnetic field, or composition, to be in proximity to zero-temperature phase transitions, or quantum critical points, QCP. This interest stems from the NFL behavior commonly found[16–24] in metals near QCP's. Many of the systems investigated, particularly those that are tuned by way of chemical substitution, are significantly disordered and the role of the disorder in determining the physical properties is not well understood.[25–30] Recent theoretical work[26–30] has focused on the emergence of Griffiths phases in disordered materials where statistically rare regions of order, or disorder, can dominate the thermodynamic response. This appears particularly relevant near zero-T phase transitions where the formation of Griffiths phases in disordered metals is thought to be the cause of the NFL behavior observed over wide regions of composition, T, and magnetic field.

In a previous paper[31] we presented, and in the accompanying article[32] expand upon, the magnetic and thermodynamic properties of the magnetic semiconductor $Fe_{1-x}Co_xS_2$ that displays features consistent with the formation of Griffiths phases.[28,29] We have demonstrated the formation of clusters of magnetic moments both at low T's for x less than x_c, the critical concentration for a long-ranged magnetic ground state, as well as above the critical temperature, T_c, for $x > x_c$. In the T range where these clusters form we find power-law T and magnetic field, H, dependencies with small exponents in agreement with that predicted for Griffiths phases.[28,29]

Here, we explore the transport properties of $Fe_{1-x}Co_xS_2$ in detail, and search for consequences of Griffiths phase formation and the emergence of long-ranged ferromagnetism, on the carrier transport. We find that Co substitution induces metallic behavior with a small density of electron-type carriers in all of our Co-doped crystals, including our most lightly doped ($x = 3 \times 10^{-4}$). For samples with $x \leq x_c$ the resistivity, ρ, and magnetoresistance, MR, are consistent with Kondo scattering of the carriers.[33–38] As we increase x beyond x_c we find that magnetic ordering produces an increasing $\rho(T)$ up to temperatures somewhat above T_c, similar to what is observed in metallic spin glasses.[39] The application of a magnetic field of 5 T dramatically reduces the resistivity of these samples by up to 35% at low temperatures. In this way the system resembles common metals with magnetic impurities with Kondo and spin glasslike anomalies.[38,39] This behavior emphasizes the interaction between the conduction electrons and the local magnetic moments associated with the Co dopants. As is true of nearly all metals that display Kondo anomalies, the resistivity of our $Fe_{1-x}Co_xS_2$ crystals

displays Fermi liquid behavior with a saturating ρ at temperatures well below the Kondo temperature, T^*.[34,38,40]

However, there is an important difference between our crystals and common Kondo systems in that $Fe_{1-x}Co_xS_2$ is a semiconductor with a small density of charge carriers and poor conduction in the range of x that we investigate. A typical figure of merit for transport in disordered metals and semiconductors is $k_F\ell$, where k_F is the Fermi wave vector of the charge carriers, and here $k_F\ell$ is between 1.5 and 15, a range typical of doped semiconductors in proximity to insulator-to-metal (IM) transitions. We observe none of the standard quantum contributions to the conductivity[7,8] that are expected in disordered Fermi liquids, instead finding that the Kondo and spin glass anomalies dominate the transport. These provide a negative MR at all fields and T's that we probe and a saturating resistivity at $T<500$ mK despite the small values of $k_F\ell$ that we infer.

There are several other peculiarities that we observe in our samples with Co concentrations closest to the critical concentration for the nucleation of a finite-temperature long-range magnetic phase. First, we have measured a very large anomalous Hall coefficient, R_S, for samples with x near x_c with R_S becoming much smaller as x is increased. The magnitude of R_S does not appear to scale with the resistivity of our samples in the manner predicted by the accepted models[41–43] of the anomalous Hall effect. In addition, we observe a residual resistivity ratio, RRR, defined as the ratio of ρ at 300 and 4 K, that is nearly 2 for all samples except those with x near x_c, where it is almost twice as large. This indicates that there is an additional T-dependent scattering mechanism beyond the typical phonon-induced carrier scattering of common metals.[44,45] We demonstrate that a simple AT^{α} dependence with $\alpha\sim 1.5$, describes $\rho(T)$ well over a large T range. The success of this simple form in modeling our data suggests that magnetic fluctuation scattering may be important over a wide T range for samples in proximity to a zero-temperature phase transition.[16,19,20,22,23,46–48]

The purpose of this paper is to present an exploration of the low T transport properties of a ferromagnetic semiconductor that displays the hallmarks of Griffiths phase formation and to highlight the differences with prototypical semiconducting systems. We provide a fuller rendering of our Hall effect, resistivity, and magnetoresistance data and analysis than that published previously.[31] This paper is organized as follows: we outline some of the important experimental details of the sample preparation, the initial characterization, and the measurement techniques in Sec. II. This is followed by a presentation of our Hall effect data and analysis in Sec. III A. The resistivity and magnetoresistance of our $Fe_{1-x}Co_xS_2$ crystals is presented in Sec. III B. Finally we summarize our results in Sec. IV.

II. EXPERIMENTAL DETAILS

Single crystals of $Fe_{1-x}Co_xS_2$ were synthesized from high-purity starting materials, including Fe powder (Alfa Aesar 99.998%), Co powder (Alfa Aesar 99.998%), and sulfur (Alfa Aesar 99.999%) as described previously.[31,32] Initial characterization included single crystal x-ray diffraction as described in Refs. 31 and 32. The lattice constant determined by the x-ray diffraction experiments[32] showed a systematic increase with Co concentration, x, in $Fe_{1-x}Co_xS_2$, beyond the lattice constant for pure FeS_2, $a=0.54165$ nm, and consistent with the measurements of Ref. 49. The increase in lattice constant with x is consistent with Vegard's law and the idea that Co replaces Fe within the pyrite crystal structure. Energy-dispersive x-ray microanalysis (EDX) on a JEOL scanning electron microscope equipped with a Kevex Si(Li) detector was performed to check the stoichiometry of our samples which were found to be consistent with the magnetic moment density determined by our dc magnetization measurements.[32] Because magnetization measurements were easily performed and highly reproducible, we have subsequently used the saturated magnetization to determine the Co concentration of our samples. Thus, throughout this manuscript the stoichiometry of the samples noted in the figures and text was determined in this manner. The variations in the saturated magnetization for crystals from the same growth batch were measured to be $\pm 10\%$ of the average value. Therefore, we report x determined from measurements of M at high field for the crystals used in each of our measurements. Wherever possible, the same crystal was employed for several different measurement types, particularly for the Hall effect and magnetization measurements used to determine anomalous Hall coefficients. As described in the accompanying article, the ac susceptibility was used to establish the magnetic phase diagram identifying Curie temperatures, T_c, and the critical Co concentration for the formation of a magnetic ground state, $x_c=0.007\pm 0.002$.[31,32]

Resistivity, magnetoresistance (MR) and Hall effect measurements were performed on single crystals polished with emery paper to an average size of $0.5\times 1\times 0.1$ mm^3. Thin Pt wires were attached to four contacts made with Epotek conductive silver epoxy. Hall effect measurements were performed at 17 or 19 Hz on samples with carefully aligned voltage leads in a Quantum Design gas flow cryostat from 1.8 to 300 K. These measurements were done in a superconducting magnet with fields ranging from −5 to 5 T and the Hall voltage, V_H, was determined as $V_H=[V(H)-V(-H)]/2$ to correct for any contamination from the field symmetric MR due to misalignment of the contacts. The resistivity and MR measurements were performed at 17 or 19 Hz using standard lock-in techniques in the Quantum Design gas flow cryostat with a 5 T superconducting magnet and a dilution refrigerator equipped with a 9 T superconducting magnet.

III. EXPERIMENTAL RESULTS

A. Hall effect

We begin our discussion of the transport properties of the charge carriers donated by the Co substitution by presenting our Hall effect measurements which give us an estimate of the charge carrier densities in our crystals. In Fig. 1(a) the Hall resistivity, ρ_{xy}, is plotted for three representative samples including our $x=0.0007$ (at 1.8 K), $x=0.007$ (at 1.8 and 10 K), and $x=0.045$ sample at a series of temperatures between 1.8 and 300 K. All samples display a negative ρ_{xy}, indicating n-type carriers, except at low H and temperatures

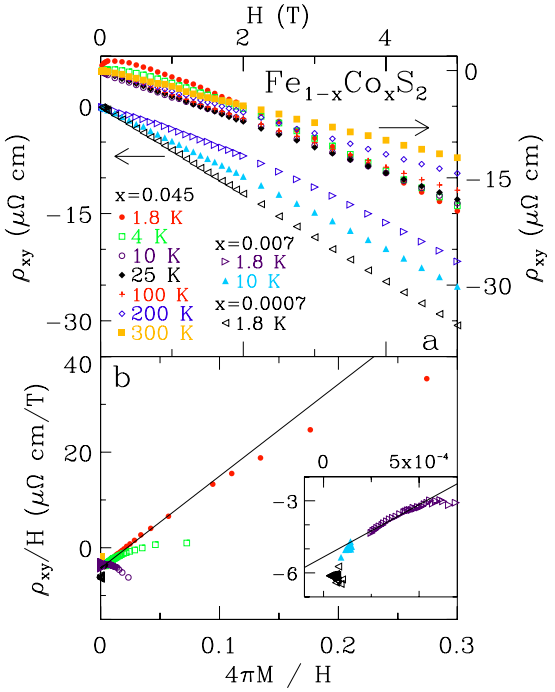

FIG. 1. (Color online) Hall resistivity. (a) The Hall resistivity, ρ_{xy}, vs magnetic field, H, at several temperatures, T, for three representative crystals with T's and x's identified in the figure. Note that the ρ_{xy} scale for the $x=0.045$ sample is on the right-hand side of the figure. (b) ρ_{xy}/H plotted as a function of the magnetization, M, divided by H to highlight the anomalous part of the Hall resistivity. Symbols are the same as in frame a. The line is a fit of a $\rho_{xy}/H=R_0+R_S(4\pi M/H)$ form to the $x=0.045$ data at 1.8 K with R_0 and R_S fitting parameters taken to be independent of H. Inset: same as frame b for $x=7\times10^{-4}$ and $x=0.007$ samples on a smaller scale. Line is a linear fit, same form as in the main frame of the figure, to the $x=0.007$ data at 4 K.

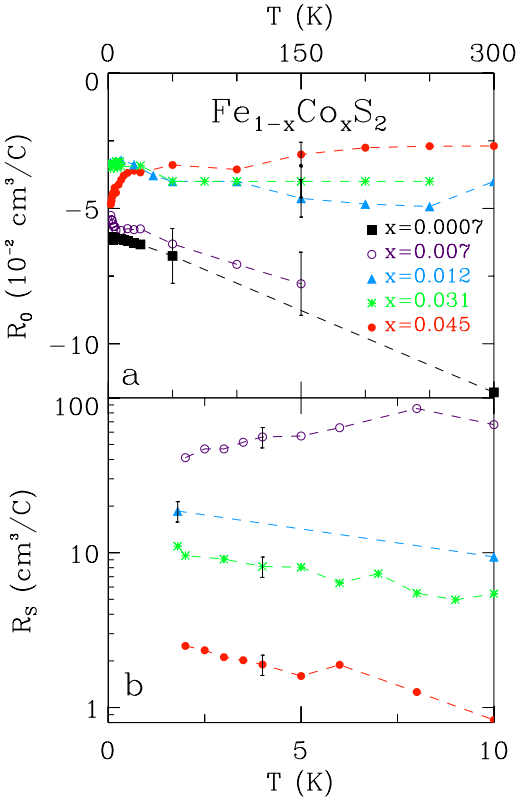

FIG. 2. (Color online) Temperature dependence of the Hall coefficients. (a) The ordinary Hall coefficient, R_0, as a function of temperature, T, for five representative crystals with x identified in the figure. R_0 is determined from fits of the Hall resistivity to the standard form $\rho_{xy}=R_0H+4\pi MR_S$ where M is the measured magnetization and R_S is the anomalous Hall coefficient. (b) Temperature dependence of R_S for four crystals identified in frame a. R_S determined with the same procedure as in frame a.

where a positive Hall potential is found for samples with $x \geq x_c$. This large positive contribution to ρ_{xy} at low fields, demonstrated in the figure for our $x=0.007$ and $x=0.045$ samples, is suppressed with T so that by warming to 10 K we again find a negative $\rho_{xy}(H)$ which is linear in H. The observation of a low-field positive contribution to ρ_{xy} is not surprising since magnetic materials typically have two contributions to their Hall resistivities, an ordinary part due to the Lorentz force experienced by the carriers proportional to H and inversely proportional to the carrier density, and an anomalous part proportional to the sample's magnetization. It is common to parameterize ρ_{xy} as

$$\rho_{xy} = R_0 H + 4\pi M R_S \tag{1}$$

with R_0 the ordinary Hall coefficient and M the magnetization, to highlight these contributions.[41–43] Interest in the anomalous Hall effect has grown over the past few years because of the large contribution it makes to ρ_{xy} in magnetic semiconductors.[3,4,13,43,50] The present understanding of the anomalous Hall effect includes contributions from extrinsic sources, due to spin-orbit scattering, and intrinsic sources, from spin-orbit effects inherent in the material's band structure.[41,43] These theories predict a strong dependence of R_S on the carrier scattering rate such that $R_S \propto \rho_{xx}^2$ for intrinsic or side jump scattering and $R_S \propto \rho_{xx}$ for skew scattering-dominated transport.[42,43]

As is standard practice, we display in Fig. 1(b) the quantity ρ_{xy}/H as a function of $4\pi M/H$ where M is the measured magnetization of these same crystals. Plotting the data in this way allows a comparison of our measured ρ_{xy} with Eq. (1). In the case where R_0 is field independent, as it is for a single carrier band, a linear M/H dependence is often found. Here we see significant curvature to ρ_{xy} indicating that there are either multiband effects in R_0, or that there is a field dependence to R_S. Field dependent R_S values are observed in materials having large MRs since the carrier-scattering rates are field dependent.[51] However, an analysis where the field dependence of the scattering rate was included explicitly was not successful in modeling the M/H dependence of ρ_{xy}/H shown in Fig. 1(b). A significant T dependence of R_S is also apparent for our $x=0.045$ sample in Fig. 1(b).

The results of parameterizing ρ_{xy} as in Eq. (1) are shown in Fig. 2 where R_0 and R_S are plotted as a function of T for five samples including the same three samples displayed in Fig. 1. R_S for our $x=0.0007$ crystal was omitted from the figure because ρ_{xy} is highly linear and the magnetization of this sample too small to allow an accurate determination. The

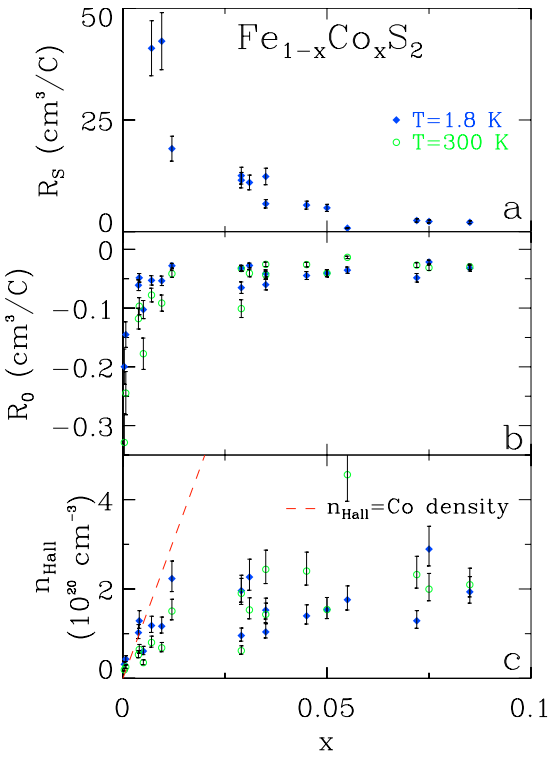

FIG. 3. (Color online) Cobalt concentration dependence of the Hall coefficients and carrier density. (a) Cobalt concentration, x, dependence of the anomalous Hall coefficient, R_S at 1.8 K. R_S was determined from fits of the form $\rho_{xy}=R_0H+4\pi MR_S$ to the Hall resistivity, ρ_{xy}, where R_0 is the ordinary Hall coefficient. (b) x dependence of R_0 determined from the same fits at 1.8 and 300 K as identified in frame a. (c) Carrier concentration, n_{Hall} determined from the simple form for the ordinary Hall coefficient, $R_0=1/n_{Hall}ec$, where e is the electronic charge and c is the speed of light, at 1.8 and 300 K as identified in frame a. Dashed line represents the carrier concentration expected if each Co dopant were to donate a single electron to a conducting band.

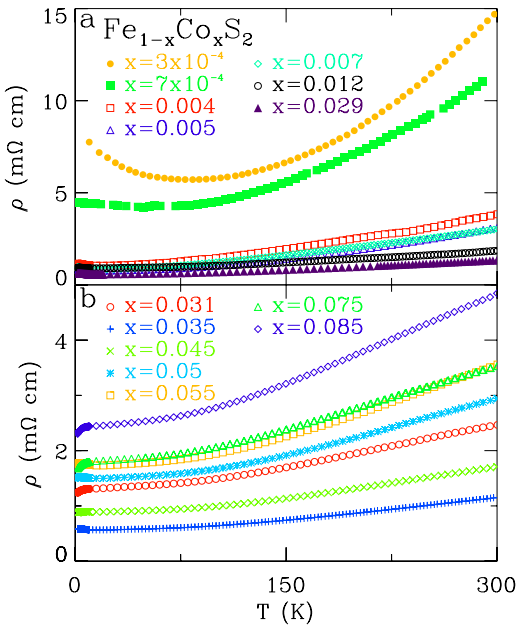

FIG. 4. (Color online) Resistivity. [(a) and (b)] Temperature, T, and cobalt concentration, x, dependence of the electrical resistivity, ρ, of several representative crystals. The stoichiometry of the crystals is identified in the figure.

T dependence of both R_0 and R_S that are apparent in Figs. 1(a) and 1(b) are made quantitative with the use of this simple form for the Hall resistivity. What is interesting, first, is the observation of significant temperature dependence of the Hall coefficients below 10 K where the magnetic susceptibility, specific heat, and, as we demonstrate below, ρ all display unusual behavior associated with the magnetic properties of these materials.[31,32] Second, we find very large R_S values for our samples that are very close to the critical point for magnetic ordering.

The x dependence of R_S and R_0 for a large number of crystals is presented in Fig. 3. Here we demonstrate the very large values of R_S found near x_c along with a continuous decrease with x beyond x_c. We note that neither the standard extrinsic nor intrinsic theories of the anomalous Hall coefficient can explain the x dependence of R_S that we measure here by way of a scattering-rate variation with x. As we demonstrate in the discussion of the resistivity below, we measure a very small variation in ρ over the range in x where the large decrease in R_S is apparent in Fig. 3(a). At present, we do not have an adequate understanding of the very large values of R_S we measure near x_c, although we speculate that an inhomogeneous magnetic state, the Griffiths phase, for $x\sim x_c$ identified from our magnetic and thermodynamic measurements, may amplify the anomalous Hall effect near x_c.[31,32] In frame c of the figure we plot the carrier density calculated from the simple form $R_0=1/n_{Hall}ec$, where n_{Hall} is the carrier density, e is the electronic charge, and c is the speed of light. We observe that n_{Hall} increases with Co substitution although it is much smaller than the Co density of these crystals, particularly for $x>0.025$. Our values of n_{Hall} indicate a carrier concentration of only 10–30 % of the Co density. Thus, there appears to be significant fraction of the electrons added by the Co substitution that are in localized states.

Our Hall data have established the sign of the charge carriers, negative as expected for Co substitution in FeS_2, and that the carrier density is only 10–30 % of the Co density of our crystals. In addition, we find very large Hall conductivities resulting from extraordinarily large anomalous Hall coefficients for samples close to the critical concentration for magnetism.

B. Resistivity

After establishing that our crystals were single phase and that Co successfully replaces Fe in FeS_2 adding electronlike carriers, we determined the resistivity, ρ, of our samples. Figure 4 shows that, although the nominally pure FeS_2 crystal is insulating, all of our crystals with Co substitutions were metallic having a ρ that extrapolates to a finite value at $T=0$.[52] Further, our crystals have ρ's that decreases with x for $x\leq 0.035$ and increase for larger x. These trends are made clearer in Fig. 5 where we plot the residual resistivity defined as ρ_0 at $T=1.8$ K. Since the Hall effect measurements pre-

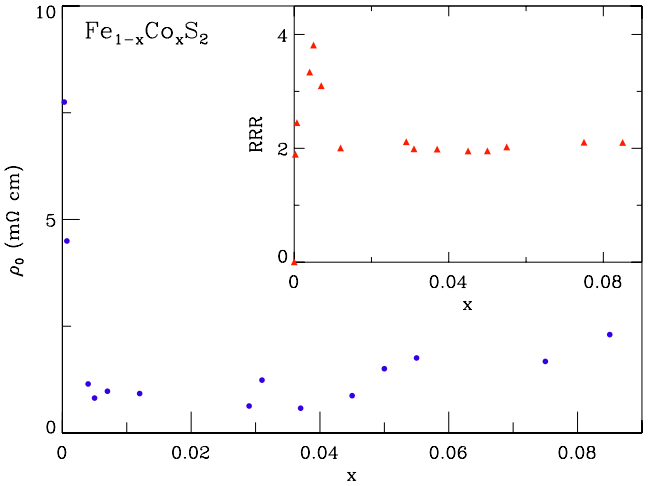

FIG. 5. (Color online) Residual resistivity and residual resistivity ratio. The residual resistivity, ρ_0, (resistivity at 4 K) of our $Fe_{1-x}Co_xS_2$ crystals. Inset; RRR, defined as the resistivity at 300 K divided by ρ_0.

sented in Sec. III A display a continuous increase in n_{Hall} with x for $x<0.025$ followed by a relatively constant carrier density at larger x, the increased ρ at $x>0.035$ indicates that the Co impurities, or other substitution-dependent defects, represent strong scattering centers for the carriers. The resistivity increases with T over most of the temperature range also indicating metallicity for all $x>0$. We summarize the T dependence of ρ by plotting the RRR of our crystals in the inset to Fig. 5. Here RRR is defined as ratio of ρ at 300 K to that at 4 K and the figure demonstrates that RRR is between 1.9 and 4 for all of our $x>0$ samples. Metals with small disorder typically display a large RRR due to a strongly T-dependent scattering rate for charge carrier-phonon scattering below the Debye temperature (Θ_D=610 K for FeS_2).[53,54] For disordered metals this dependence can be hidden by a large impurity, T-independent, scattering rate. In our samples, the RRR is small, a second indication that the impurities and defects related to the chemical substitution represent strong scattering centers for the doped carriers. In addition to the impurity-related scattering and the phonon scattering apparent in the resistivity, there appears to be a separate, T-dependent, contribution to ρ of our crystals evident below ~20 K.

1. Resistivity below 20 K

The temperature dependence of the charge carrier transport at low T's can often reveal much about the character of the charge carriers and their scattering. Therefore we have explored the carrier transport below 20 K in some detail as shown in Figs. 6 and 7 where we display ρ of a few representative crystals. As these figures demonstrate, crystals with $x<0.01$ generally display a decreasing ρ with T below 20 K while those with $x>0.01$ display an increasing ρ with T leading to a maximum in ρ at temperatures somewhat above T_c.[32] In addition, we observe that ρ tends toward saturation by $T<0.3$ K, a behavior typically observed in metals without substantial disorder where it is indicative of transport in

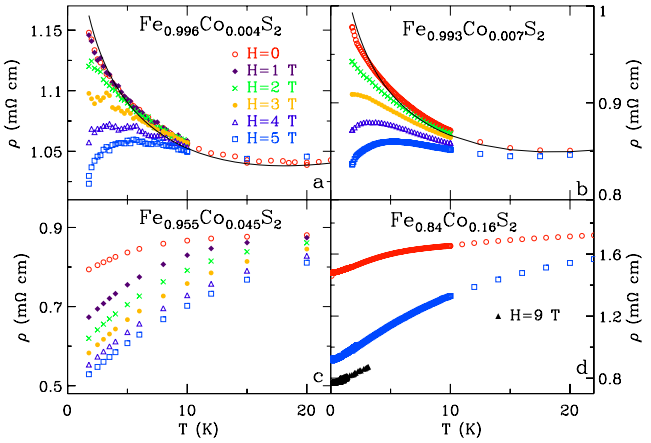

FIG. 6. (Color online) Resistivity and Magnetoresistance. [(a)–(d)] Temperature, T, dependence of the resistivity, ρ of four single crystals at magnetic fields, H, and stoichiometry's identified in the figure. Zero-field data same as in Fig. 4. Solid line is a fit of a Kondo anomaly form to the data using the Kondo temperature determined from a scaling of the magnetoresistance data (see text) (Ref. 34).

a Fermi liquid. The resistivities we measure are above 500 $\mu\Omega$ cm, consistent with the small carrier concentration revealed in our Hall effect measurements and a large scattering rate. A typical measure of the proximity to the insulator-to-metal transition is the quantity $k_F\ell$, where k_F is the Fermi wave vector and ℓ is the mean-free path of the carriers. Our estimates of $k_F\ell$ at 4 K for the samples shown in Fig. 4 range

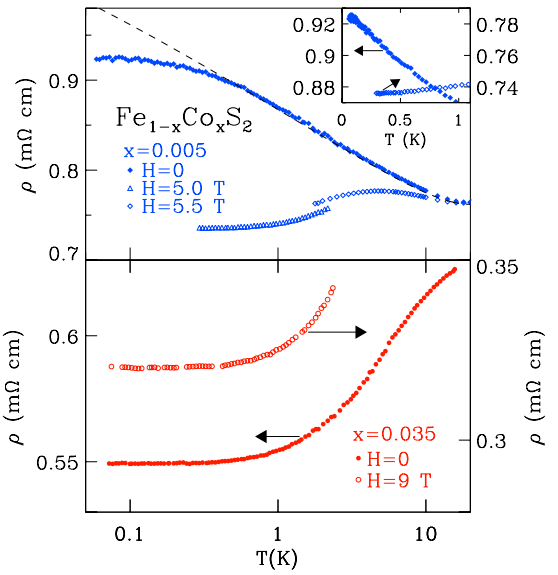

FIG. 7. (Color online) Low-temperature resistivity. The resistivity, ρ, as a function of temperature, T, at $0.07<T<20$ K for two representative crystals with (a) x=0.005 and (b) x=0.035. Magnetic fields are identified in the figure. Dashed line in frame "a" is a fit of the Kondo form (Ref. 34) to the data above 0.5 K with the Kondo temperature held at 1.4 K as determined from the best scaling of the magnetoresistance data. See text for details. Inset: same data as in frame a, highlighting the variation in ρ below 1 K. Symbols are the same as in the main frame.

from 1.5 for our smallest x, to 15 for the crystals having the smallest ρ_0 in Fig. 5.

As is apparent in Figs. 6 and 7 the application of magnetic fields substantially decreases ρ for all samples measured, independent of the sign of $d\rho/dT$. The decrease in resistivity is as large as 35% of ρ_0 for a 5 T field. The negative MR we observe is at odds with what has been measured in common semiconductors such as Si:P and other magnetic semiconductors, such as $Fe_{1-x}Co_xSi$, where a positive MR is associated with the electron-electron interaction effects.[9,11,12] For samples that display a $d\rho/dT<0$ at $H=0$ the effect of magnetic field is to reverse the sign of the temperature derivative so that all samples have a $d\rho/dT>0$ at high fields. Instead of resembling the transport of charge carriers in prototypical semiconductors, we observe a behavior similar to what is seen when magnetic impurities are added to high-purity metals.[38]

In common metals the addition of magnetic impurities leads to a low T resistivity anomaly that has been extensively investigated[33,38] for over 40 years. Small impurity densities, typically less than 0.01%, induce an increased ρ with decreasing T similar to what we observe here. This is the well-known Kondo effect[33,38] where conduction electrons increasingly screen the magnetic impurities as the temperature is lowered. The effect of a magnetic field is to Zeeman split the energy levels of the impurity moments effectively removing the Kondo resonance, thereby removing a scattering channel for the carriers. At higher impurity concentrations, interactions between impurity magnetic moments become of the same order as the effective screening temperature, k_BT^*, where k_B is Boltzmann's constant. In this case, a spin glass or a disordered magnetic state forms at low T and is typically indicated by a decrease in ρ below the glass freezing or magnetic-ordering temperature.[39] We note that the T and x ranges where we observe $d\rho/dT>0$ at $H=0$ correspond well with the magnetically ordered states identified by a peak in the ac susceptibility.[32]

In Figs. 6 and 7 we have included a comparison of our data for $\rho(T)$ at $H=0$ with a standard form for the Kondo resistance anomaly given by Hamann[34,35]

$$\rho_{spin} = S\rho_0\left\{1-\cos 2\delta_\nu \frac{\ln T/T_K}{[\ln^2 T/T_K + \pi^2 S(S+1)]^{1/2}}\right\}, \quad (2)$$

where T_K is the Kondo temperature, S the spin of the impurity, δ_ν the phase shift due to ordinary scattering, and ρ_0 the s-wave unitarity limit resistivity. We have fit this form to our data for $x<x_c$ with S set at 1/2 and T_K held at the value of T^* found from the scaling of the MR, see below, and found best fit values for δ_ν between 25° and 60°.

The field dependence of ρ at constant T for the same four crystals as in Fig. 6 is shown in Fig. 8 where the negative MR is once again displayed. The size of the MR decreases with temperature so that by about $T=25$ K there is only a small MR (<5%). The MR at 1.8 K is large indicating that the scattering of the carriers by the magnetic impurities is dominating ρ of our crystals, particularly at larger x. We also observe a change in the shape of the MR at low H for $x>0.01$. Although the MR is negative and analytic at $H=0$ for samples with $x<x_c=0.007\pm0.002$, as well as for $x>x_c$ at

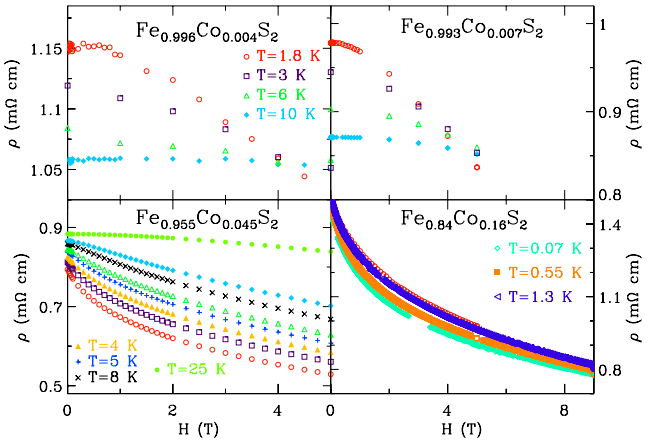

FIG. 8. (Color online) Magnetoresistance. [(a)–(d)] The magnetoresistance (resistivity, ρ as a function of magnetic field, H) for the same crystals as in Fig. 6 with stoichiometry's and temperatures, T, identified in the figure. The current direction was perpendicular to H, transverse MR, for all data presented in the figure.

$T>T_c$, it is very sharp at $T<T_c$, a feature commonly observed in ferromagnetic metals.[55]

A common indicator for the mechanism of the MR is the difference in MR for currents parallel and perpendicular to the magnetic field. In Fig. 9 we plot the MR measured for two representative samples in the two current-field configurations. We have chosen one sample with $x<x_c$ and one with $x>x_c$ for this plot, and in both cases there is little change in the MR with field orientation. We conclude that the contributions to the MR from orbital effects is minimal in agreement with our tentative assignment of the MR, and T-dependent ρ, to a Kondo anomaly.

To further test the hypothesis that the MR is related to scattering from magnetic moments associated with the Co substitution, and more specifically the Kondo effect for $x<x_c$, we have attempted a simple scaling of the MR to a

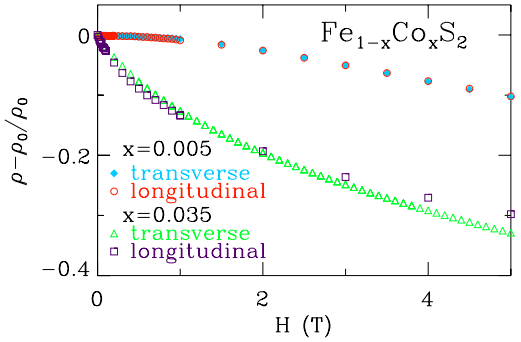

FIG. 9. (Color online) Transverse and longitudinal magnetoresistance. (a) The MR, defined as the resistivity, ρ, as a function of magnetic field, H after subtracting the resistivity at $H=0$, ρ_0, and dividing by ρ_0, $\rho-\rho_0/\rho_0$, of two representative crystals at 1.8 K. Stoichiometry's of the crystals are identified in the figure. The longitudinal MR refers to the current direction being parallel to H. The transverse MR refers to the measurement geometry where the current is in the same direction with respect to the crystal as in the longitudinal MR measurement but with the crystal oriented such that the current is perpendicular to H.

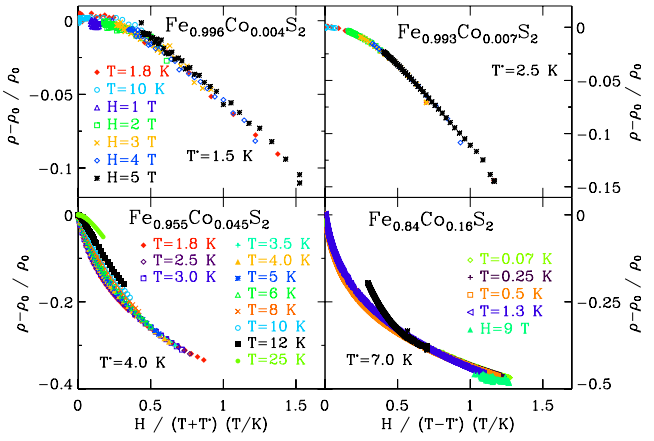

FIG. 10. (Color online) Scaling plot of the magnetoresistance. [(a)–(d)] Magnetoresistance, $\rho-\rho_0/\rho_0$ where ρ is the resistivity and ρ_0 refers to the resistivity in zero magnetic field, H, as a function of H divided by the temperature, T, added to the Kondo temperature, T^* determined by the best scaling of the these data. The stoichiometry of the crystals is indicated in the figure, as is the value of T^* which leads to the best scaling of the data. T and H for the constant temperature and field scans are indicated in the figure. The scaling is seen to work well for samples where $x<x_c$, the critical Co concentration for ferromagnetism, frames a and b. In frames c and d where $x>x_c$, no value of T^* results in reasonable scaling of all the data.

standard Kondo form, $(\rho-\rho_0)/\rho_0=f[H/(T+T^*)]$.[36,37] In Fig. 10 we display the typical results of our scaling procedure for crystals with $0.004\leq x\leq 0.16$. While the scaling quality is within the scatter of the data for paramagnetic samples, $x<x_c=0.007$, there is significant deviation from scaling for samples having a magnetic transition at finite T. The values for T^* resulting in the best scaling of our data are plotted in Fig. 11 where T^* is seen to increase with x. We conclude from the quality of the scaling of the data that a single-ion Kondo form does well to describe the resistivity where the interaction between moments is expected to be small, that is,

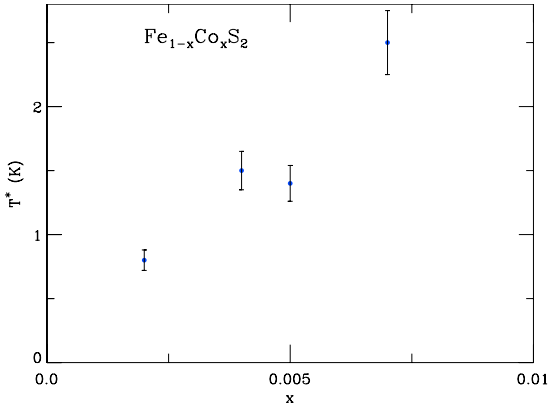

FIG. 11. (Color online) Kondo temperature. The Co concentration dependence, x of the Kondo temperature T^* as determined from scaling of the magnetoresistance, see Fig. 10, for example. Only samples where x is less than the critical concentration for ferromagnetism, x_c, is T^* accurately determined and only those data are plotted in the figure.

for $x\leq x_c$ and T larger than a scale related to the interactions between local moments, such as an RKKY energy scale. This is in accord with our magnetization measurements for samples with $x<x_c$ where the T dependence of the magnetic susceptibility displays a small negative Weiss T.[31,32] From the quality of the fits shown in the figures, and the quality of the scaling of the MR in Fig. 10, we conclude that a single-ion Kondo form describes the low-temperature transport of our samples with $x<x_c$ well, while for $x>x_c$ the transport properties resemble those of Kondo systems where the concentration of magnetic impurities is large enough so that interaction between them results in magnetic ordering.

Since $k_F\ell$ is close to 1 in our crystals, we expect that ρ display evidence of electron-electron interaction effects that dominate the low-T magnetotransport of prototypical semiconductors,[7–9] and some magnetic semiconductors,[12,15] near the IM transition. The resistivity of common semiconductors with doping concentrations near that required for a IM transition display both a $T^{1/2}$ dependence at low T and a positive MR that grows as $H^{1/2}$ for $g\mu_B H>k_B T$. We observe, instead, resistivities that, below 1 K, appear to be a continuation of the Kondo or spin glasslike forms in Figs. 6 and 7 so that neither of these signatures of quantum interference is obvious in $Fe_{1-x}Co_xS_2$. In this same range of x and T, our specific heat and magnetic susceptibility measurements reveal the formation of Griffiths phases which have been suggested to be a cause of non-Fermi-liquid behavior.[26,28,31,32] Instead, we observe a saturating resistivity below 1 K most straightforwardly interpreted as Fermi-liquid behavior.

2. Resistivity above 20 K

Above 20 K the resistivity shown in Fig. 4 increases with increased T demonstrating metallic conduction of the carriers introduced by Co substitution. However, the thermally induced scattering does not increase ρ of our crystals by more than a factor of 2 in most crystals (see RRR in Fig. 5) reflecting the importance of the substitutional disorder.

The resistivity of a few representative samples is shown in Figs. 12(a) and 12(b) where the temperature dependence of the resistivity appears to be almost linear over a wide range of temperatures. In the usual description of metallic transport, based in part on Matthiessen's rule, carrier scattering due to impurities is considered T independent while the scattering from the thermally activated phonons is highly T dependent. The standard,[44,45] semiclassical, Debye treatment of carrier-phonon scattering predicts a $\rho\propto(T/\Theta_D^\rho)^5$ behavior for $T<\Theta_D^\rho$ evolving into a $\rho\propto T/\Theta_D^\rho$ form for $T>\Theta_D^\rho$. Here Θ_D^ρ is the transport Debye temperature. The Debye temperature for iron pyrite is 610 K (Ref. 53) and we estimate the transport Debye temperature, $\Theta_D^\rho=2\hbar k_F s/k_B$, where s is the speed of sound (8980 m/s), to be between 200 and 250 K.[45,56] Although in magnetic materials the higher T resistivity is difficult to model because of contributions from phonon and magnetic scattering are difficult to separate, we find that the Debye form adequately describes the resistivity of our samples over a wide range of T with a few notable exceptions. In particular, for samples with x close to x_c, the model deviates substantially from the data near 50 K, as

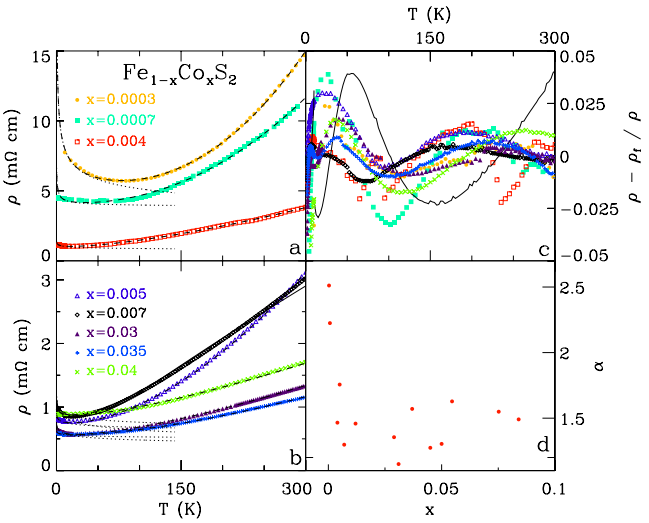

FIG. 12. (Color online) Temperature dependence of the resistivity. (a) The resistivity, ρ for three crystals with Co concentrations, x indicated in the figure. Dashed lines are fits of a model that includes a residual resistivity, ρ_0 added to a Kondo anomaly and a simple power law form, AT^{α}. The Kondo form was determined from fits to the low-temperature resistivity ($T<10$ K), for example, see Fig. 6 and displayed below 150 K by the dotted lines in the figure. (b) ρ for five representative crystals with x's indicated in the figure. Dashed and dotted lines are the same as in frame a. Solid line is a fit of a Debye model to the $x=0.007$ data. (c) $\rho-\rho_f/\rho$, deviation of the resistivity from the fits, ρ_f, showing that for crystals with x in proximity to x_c a power law form with $\alpha=1.6\pm0.1$ describes the data well over an extended temperature range. Solid line is $\rho-\rho_{fd}/\rho$ where ρ_{fd} represents the fit of the Debye model to the resistivity of the $x=0.007$ crystal. (d) α as determined from fits of the model to the data in frames a and b.

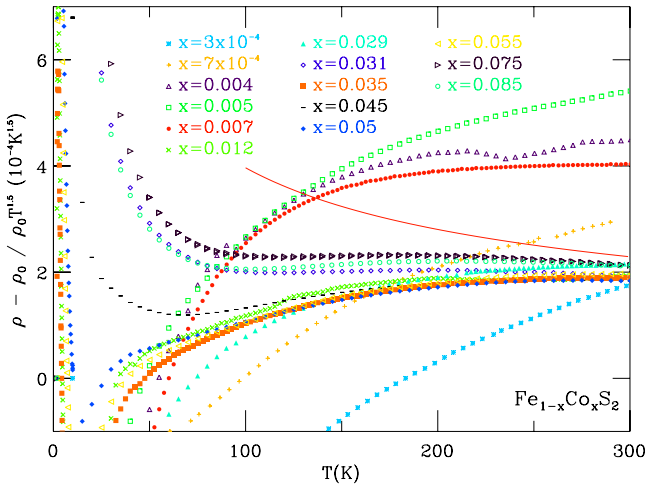

FIG. 13. (Color online) Reduced resistivity. (a) The resistivity, ρ, after subtraction of the resistivity at 4 K, ρ_0, normalized by ρ_0 and divided by $T^{1.5}$ vs temperature, T, for 14 representative crystals with x's identified in the figure. All samples except those with x nearest to x_c have values that approach 2×10^{-4} $\mathrm{K}^{-1.5}$ while those with $x\sim x_c$ display values larger than 4×10^{-4} $\mathrm{K}^{-1/5}$. The red line in the figure represents a linear temperature dependence, such as that expected for phonon scattering at T larger than the Debye temperature.

demonstrated for our $x=0.007$ sample in Figs. 12(b) and 12(c).

We have considered a simple alternative to the standard phonon-scattering model of resistivity motivated by our observation that the resistivity data appear to have a nearly linear T dependence over a wide range in T. This alternative, demonstrated in Fig. 12, consists of a simple power-law form, $\rho=\rho_0+AT^{\alpha}$, added to the same Kondo description of the low-T data (Eq. (2)) as in Fig. 6. The results of this procedure where α, A, and ρ_0 are allowed to vary is represented in frames a and b of Fig. 12 by the dashed lines. The ability of such a simple model to reproduce the data is remarkable. In fact, the difference between the data and model shown in frame c of Fig. 12 is smaller for samples with $x\sim x_c$ than the much more complex Debye model, demonstrated by the solid line in the figure, although some systematic differences remain below 100 K. The best-fit values of the temperature exponent, α, are shown in frame d where α is seen to change from about 2.5 for small x ($x=3\times10^{-4}$) to values between 1.2 and 1.6.

Why such a simple expression does such an accurate job of describing our resistivity data is not clear. However, we suggest that the formation of a magnetically ordered state at low T implies that scattering from magnetic fluctuations plays an important role in determining $\rho(T)$. The large reduction of ρ_0 by the application of moderately sized magnetic fields, a decrease of 45% of ρ_0 with a 9 T field as seen in Fig. 8, supports the idea that magnetic scattering is a substantial fraction of ρ_0. Our observations that the RRR$\approx$4 for samples near x_c and the that the quality of fits of a simple power-law temperature dependence to $\rho(T)$ indicate magnetic fluctuations to be an important contribution to the carrier scattering in this range of x over a wide temperature range.

The simple power-law analysis of $\rho(T)$ at $T>20$ K has demonstrated that the resistivity of our samples closely resembles a $\rho=\rho_0+AT^{\alpha}$ dependence with $\alpha\approx1.5\pm0.1$ in a wide range of x and T. In order to assess the systematics and validity of this model we have plotted the quantity $(\rho-\rho_0)/(\rho_0*T^{1.5})$ in Fig. 13. In this way we can compare scattering rates in samples with very different carrier concentrations and remove the error associated with the measurement of the geometry of our crystals. If the power-law expression were to strictly hold, this quantity would yield the parameter A divided by ρ_0. Dividing by ρ_0 normalizes A by eliminating the simple effects of carrier concentration and impurity scattering rate changes with x. Thus, the figure isolates the magnitude of this quantity related to the T-dependent part of the scattering rate of the carriers. The figure demonstrates that this value is very closely clustered about $(\rho-\rho_0)/(\rho_0T^{1.5})=2\times10^{-4}$ $\mathrm{K}^{-1.5}$ for nearly all of our samples. The obvious exceptions are the crystals with x nearest to x_c on the paramagnetic side where a value of 4×10^{-4} to 6×10^{-4} $\mathrm{K}^{-1.5}$ is found, reflecting the observation of a much larger RRR in these samples.

It appears from this simple analysis that the T-dependent scattering rate above $\sim$150 K is extraordinarily independent of x for $x>x_c$ while is at least twice as large for $x\simeq x_c$. From this we conclude that there is a carrier scattering mechanism

that is enhanced very near the critical concentration for magnetism in this system. Given the power-law-like dependence on T, we assert that carrier scattering from magnetic fluctuations contributes a significant fraction of the resistivity over the entire temperature range we measure.

Resistivities, and thus by implication charge carrier scattering rates, that display similar temperature-dependent power-law behaviors for $T<20$ K have been documented for nearly ferromagnetic and weakly ferromagnetic metals such as $Pd_{1-x}Ni_x$ (Ref. 46) and $ZrZn_2$,[19] where scattering from spin fluctuations produces a $T^{5/3}$ dependence of ρ. This behavior is observed in highly itinerant magnets where a Stoner-Wholfarth model of magnetism[48] is appropriate and is thought to signify the emergence of a marginal Fermi-liquid ground state.[57] Other materials in this category, being weakly ferromagnetic and in proximity to a QCP, are well known for having power-law T-dependent resistivities, $\rho=\rho_0+AT^{\alpha}$, with small α (between 1 and 1.5), for $T<10$ K, include MnSi under pressure,[17,20] $Ce(Cu_{1-x}Au_x)_6$,[22] and $YbRh_2Si_2$.[16] None of these examples display power-law behavior above about 20 K. One exception is the high-temperature superconducting oxides of copper where $\rho \propto T^{1.5}$ has been documented for overdoped samples of $La_{2-x}Sr_xCuO_4$ over an enormous temperature range.[23] How the temperature-dependent resistivity of $Fe_{1-x}Co_xS_2$ we observe here fits into this evolving story is not clear. However, we point out that all of these materials reside near a magnetic phase transition that has been tuned toward zero temperature.

Since we have previously demonstrated that the magnetic and thermodynamic properties of this system have power-law T dependencies that are due to formation of Griffiths phases, it is natural to consider if carrier scattering from these excitations is responsible for the $T^{1.5}$ behavior of the resistivity we measure. The Griffiths phases consist of finite-sized regions of incipient magnetic order fluctuating in time where exponentially large, rare, regions can dominate the thermodynamic response. The density of clusters with excitation energies less than k_BT can be easily calculated to have a T^{λ} dependence where $\lambda \sim 1/2$ leading to a scattering rate for charge carriers of the same form.[27,28] Therefore, in order to explain the T dependence of the resistivities we measure with this mechanism, we would have to assume matrix element effects, most likely due to the finite sizes of the rare regions, that would enhance the temperature-dependent scattering to a $\sim T^{1.5}$ form.

IV. DISCUSSION AND CONCLUSIONS

In $Fe_{1-x}Co_xS_2$ we have previously observed that the Co dopants each contribute localized magnetic moments to the diamagnetic insulator FeS_2.[31,32,52] These moments tend to form magnetic clusters and at low T we have observed the emergence of a disordered ferromagnetic phase at $x_c=0.007\pm0.002$. The thermodynamic and magnetic properties we measure indicate the presence of Griffiths phases.[31,32] Our Hall effect data presented here reveal a density of electrical carriers of only 10–30 % of the Co concentration indicating a substantial localization of electrons donated by the Co substitution. A slight curvature evident in the plots of the Hall potential vs the magnetic field may indicate the existence of a small population of compensating holes. The reasons for the low carrier densities are not clear at this time but may reflect a significant substitutional-related disorder. In the magnetically ordered samples we observe an anomalous Hall effect with a very large coefficient (R_S) which decreases with x.

Measurements of the low-T resistivity show that the charge carriers interact substantially with the magnetic moments in this system. We have presented evidence that the Kondo effect dominates the carrier transport for $x \leq x_c$ for $T<10$ K and, as is the case for both simple metals with magnetic impurities and Kondo lattice systems,[34,38,40] the resistivity saturates at low T. We point out that the carrier densities estimated from the Hall effect are sufficient to screen only a small fraction of the doping-induced magnetic moments, leaving the system highly underscreened or undercompensated. The saturating temperature-dependent ρ at the lowest T's indicate a Fermi-liquid ground state with contributions from quantum interference effects commonly found in doped semiconductors not observed.

Despite the interesting magnetic and thermodynamic properties we measure, including power-law temperature dependencies down to very low T, we observe no indication of NFL behavior in the transport properties of our $Fe_{1-x}Co_xS_2$ crystals. Thus, just as in the prototypical semiconducting systems such as phosphorous-doped silicon,[58–60] NFL behavior observed in the magnetic and thermodynamic properties that persist into the metallic side of the IM transition, does not lead to NFL charge transport. In Si:P, where disordered Fermi-liquid transport is observed,[58] the implication is that the conducting electrons and the more localized dopants which dominate the magnetization and specific heat, C, only interact weakly. It has even been postulated that these two electron fluids reside in physically separate regions of the disordered semiconductor. In contrast, in $Fe_{1-x}Co_xS_2$, we find convincing evidence that the conducting electrons and the localized electrons responsible for the magnetic properties of these materials interact substantially. The Kondo resistance anomaly, so clearly defined in our data, indicates the importance of such an interaction. Yet, perhaps surprisingly, we do not observe any indication of NFL behavior in the charge carrier transport to the lowest temperatures measured despite ample evidence for NFL response of $M(H,T)$ and $C(H,T)$.[31,32]

The low-temperature transport properties of $Fe_{1-x}Co_xS_2$ we outline above are substantially different from those of Co and Mn substituted FeSi, a second magnetic semiconducting system where detailed low-T measurements have been carried out.[12,13,15] While both of the nominally pure compounds, FeS_2 and FeSi, have small band gaps and are nonmagnetic having very small magnetic susceptibilities, both become magnetic upon electron doping via Co substitution. However, electron doping of FeSi results in a highly itinerant helimagnetic ground state where standard quantum contributions to the conductivity are dominant. Clearly this is distinct from what we measure here in $Fe_{1-x}Co_xS_2$. Hole doping FeSi by way of Mn substitution is similar to $Fe_{1-x}Co_xS_2$ in that it was found to display undercompensation.[15] In this case, the Mn dopants contribute a spin-1 moment and a single spin-1/2

hole carrier. The resistivity of these compounds remained T dependent down to the lowest temperatures, however, the temperature dependence was not the $T^{1/2}$ behavior found in standard semiconducting systems such as Si:P.[9,11] The NFL behavior discovered in $Fe_{1-x}Mn_xSi$ is in agreement with calculations predicting a singular Fermi liquid in the undercompensated Kondo model.[61–64] In addition, the application of modest magnetic fields reduces the inelastic scattering and restores the typical temperature and field dependencies expected for quantum interference effects.[12] We remain puzzled as to the cause of dramatic differences in the transport properties of these, naively similar, magnetic semiconducting systems.

Finally, the temperature dependence of the resistivity in the T range where phonon scattering dominates the ρ of typical metals shows some peculiarities. In particular, the temperature dependence of the resistivity is enhanced for samples with x very near x_c, having a RRR twice as large as samples on either side of x_c. Although a semiclassical model of carrier-phonon scattering describes the broad features of $\rho(T)$ our models show systematic differences with the data below 100 K for the samples with $x \sim x_c$. We have demonstrated that a simple power-law form surprisingly describes the data at least as well as the semiclassical model[44,45] in this range of x. We speculate that the resistivity of these compounds results, in part, from magnetic fluctuation scattering of the carriers, even at temperatures approaching room T.

In summary, Co doping of FeS_2 adds both local magnetic moments and electron charge carriers to this band-gap insulator. Our data indicate that although the magnetic and thermodynamic properties of $Fe_{1-x}Co_xS_2$ for $0 \leq x \leq 0.085$ are dominated by the presence of Griffiths phases at low temperatures, the transport is Fermi liquidlike. It appears that there is a Kondo coupling of the carriers and local magnetic moments that produces a saturating resistivity below ~ 0.3 K. Despite the small mean-free path of the doped charge carriers we observe no indication of quantum corrections to the conductivity. Thus, despite the NFL behavior found in the magnetic and thermodynamic properties, we observe transport properties that can be described as dominated by Kondo anomalies, and/or magnetic scattering, but are essentially Fermi liquidlike.

ACKNOWLEDGMENTS

We thank I. Vekhter and C. Capan for discussions. J.F.D., D.P.Y., and J.Y.C. acknowledge support of the NSF under Grants No. DMR084376, No. DMR0449022, and No. DMR0756281.

[1] S. A. Wolf, D. D. Awschalom, R. A. Buhrman, J. M. Daughton, S. von Molnar, M. L. Roukes, A. Y. Chtchelkanova, and D. M. Treger, Science **294**, 1488 (2001).
[2] S. Von Molnar and D. Read, Proc. IEEE **91**, 715 (2003).
[3] H. Ohno, A. Shen, F. Matsukura, A. Oiwa, A. Endo, S. Katsumotos, and Y. Iye, Appl. Phys. Lett. **69**, 363 (1996).
[4] H. Ohno, H. Munekata, T. Penney, S. von Molnar, and L. L. Chang, Phys. Rev. Lett. **68**, 2664 (1992).
[5] F. Matsukura, H. Ohno, A. Shen, and Y. Sugawara, Phys. Rev. B **57**, R2037 (1998).
[6] M. L. Reed, N. A. El-Masry, H. H. Stadelmaier, M. K. Ritums, M. J. Reed, C. A. Parker, J. C. Roberts, and S. M. Bedair, Appl. Phys. Lett. **79**, 3473 (2001).
[7] B. L. Al'tshuler, A. G. Aronov, M. E. Gershenson, and Yu. V. Sharvin, Sov. Sci. Rev., Sect. A **9**, 223 (1987).
[8] P. A. Lee and T. V. Ramakrishnan, Rev. Mod. Phys. **57**, 287 (1985).
[9] T. F. Rosenbaum, R. F. Milligan, M. A. Paalanen, G. A. Thomas, R. N. Bhatt, and W. Lin, Phys. Rev. B **27**, 7509 (1983).
[10] T. F. Rosenbaum, R. F. Milligan, G. A. Thomas, P. A. Lee, T. V. Ramakrishnan, R. N. Bhatt, K. DeConde, H. Hess, and T. Perry, Phys. Rev. Lett. **47**, 1758 (1981).
[11] S. Bogdanovich, P. H. Dai, M. P. Sarachik, V. Dobrosavljevic, and G. Kotliar, Phys. Rev. B **55**, 4215 (1997).
[12] N. Manyala, Y. Sidis, J. F. DiTusa, G. Aeppli, D. P. Young, and Z. Fisk, Nature (London) **404**, 581 (2000).
[13] N. Manyala, Y. Sidis, J. F. DiTusa, G. Aeppli, D. P. Young, and Z. Fisk, Nature Mater. **3**, 255 (2004).
[14] F. P. Mena, J. F. DiTusa, D. van der Marel, G. Aeppli, D. P. Young, A. Damascelli, and J. A. Mydosh, Phys. Rev. B **73**, 085205 (2006).
[15] N. Manyala, J. F. DiTusa, G. Aeppli, and A. P. Ramirez, Nature (London) **454**, 976 (2008).
[16] J. Custers, P. Gegenwart, H. Wilhelm, K. Neumaier, Y. Tokiwa, O. Trovarelli, C. Geibel, F. Steglich, C. Pepin, and P. Coleman, Nature (London) **424**, 524 (2003).
[17] N. D. Mathur, F. M. Grosche, S. R. Julian, I. R. Walker, D. M. Freye, R. K. W. Haselwimmer, and G. G. Lonzarich, Nature (London) **394**, 39 (1998).
[18] Q. M. Si, K. Ingersent, and J. L. Smith, Nature (London) **413**, 804 (2001).
[19] R. P. Smith, M. Sutherland, G. G. Lonzarich, S. S. Saxena, N. Kimura, S. Takashima, M. Nohara, and H. Takagi, Nature (London) **455**, 1220 (2008).
[20] N. Doiron-Leyraud, I. R. Walker, L. Taillefer, M. J. Steiner, S. R. Julian, and G. G. Lonzarich, Nature (London) **425**, 595 (2003).
[21] G. R. Stewart, Rev. Mod. Phys. **73**, 797 (2001).
[22] A. Schröder, G. Aeppli, R. Coldea, M. Adams, O. Stockert, H. v. Löhneysen, E. Bucher, R. Ramazashvili, and P. Coleman, Nature (London) **407**, 351 (2000).
[23] H. Takagi, B. Batlogg, H. L. Kao, J. Kwo, R. J. Cava, J. J. Krajewski, and W. F. Peck, Phys. Rev. Lett. **69**, 2975 (1992).
[24] J. S. Kim, J. Alwood, G. R. Stewart, J. L. Sarrao, and J. D. Thompson, Phys. Rev. B **64**, 134524 (2001).
[25] R. B. Griffiths, Phys. Rev. Lett. **23**, 17 (1969).
[26] A. H. Castro Neto, G. Castilla, and B. A. Jones, Phys. Rev. Lett. **81**, 3531 (1998).
[27] A. H. Castro Neto and B. A. Jones, Phys. Rev. B **62**, 14975 (2000).
[28] E. Miranda and V. Dobrosavljevic, Rep. Prog. Phys. **68**, 2337

(2005).
[29] T. Vojta, J. Phys. A **39**, R143 (2006).
[30] A. J. Millis, D. K. Morr, and J. Schmalian, Phys. Rev. B **66**, 174433 (2002).
[31] S. Guo, D. P. Young, R. T. Macaluso, D. A. Browne, N. L. Henderson, J. Y. Chan, L. L. Henry, and J. F. DiTusa, Phys. Rev. Lett. **100**, 017209 (2008).
[32] S. Guo, D. P. Young, R. T. Macaluso, D. A. Browne, N. L. Henderson, J. Y. Chan, L. L. Henry, and J. F. DiTusa, preceding paper, Phys. Rev. B **81**, 144423 (2010).
[33] J. Kondo, Prog. Theor. Phys. **32**, 37 (1964).
[34] D. R. Hamann, Phys. Rev. **158**, 570 (1967).
[35] J. S. Schilling, Adv. Phys. **28**, 657 (1979).
[36] P. Schlottmann, Phys. Rep. **181**, 1 (1989).
[37] B. Andraka and G. R. Stewart, Phys. Rev. B **49**, 12359 (1994).
[38] C. Rizzuto, Rep. Prog. Phys. **37**, 147–229 (1974).
[39] J. S. Schilling, P. J. Ford, U. Larsen, and J. A. Mydosh, Phys. Rev. B **14**, 4368 (1976).
[40] Z. Fisk, J. L. Sarao, J. L. Smith, and J. D. Thompson, Proc. Natl. Acad. Sci. U.S.A. **92**, 6663 (1995).
[41] J. M. Luttinger, Phys. Rev. **112**, 739 (1958).
[42] F. E. Maranzana, Phys. Rev. **160**, 421 (1967).
[43] T. Jungwirth, Q. Niu, and A. H. MacDonald, Phys. Rev. Lett. **88**, 207208 (2002).
[44] See, e.g., J. M. Zimon, *Electrons and Phonons: The Theory of Transport Phenomena in Solids*, (Oxford University Press, London, 1960).
[45] V. F. Gantmakher and Y. B. Levinson, *Carrier Scattering in Metals and Semiconductors* (North-Holland, Amsterdam, 1987).
[46] M. Nicklas, M. Brando, G. Knebel, F. Mayr, W. Trinkl, and A. Loidl, Phys. Rev. Lett. **82**, 4268 (1999).
[47] C. Pfleiderer, S. R. Julian, and G. G. Lonzarich, Nature (London) **414**, 427 (2001).
[48] See, e.g., T. Moriya, in *Spin Fluctuations in Itinerant Electron Magnetism*, edited by P. Fulde (Springer, Berlin, 1985).
[49] R. J. Bouchard, Mater. Res. Bull. **3**, 563 (1968).
[50] H. Ohno, J. Magn. Magn. Mater. **200**, 110 (1999).
[51] M. Lee, Y. Onose, Y. Tokura, and N. P. Ong, Phys. Rev. B **75**, 172403 (2007).
[52] H. S. Jarrett, W. H. Cloud, R. J. Bouchard, S. R. Butler, C. G. Fredric, and J. Gillson, Phys. Rev. Lett. **21**, 617 (1968).
[53] R. A. Robie and J. L. Edwards, J. Appl. Phys. **37**, 2659 (1966).
[54] J. Kansy, T. J. Panek, and M. Szuszkiewicz, J. Phys. C **17**, 1585 (1984).
[55] See, e.g., I. A. Campbell and A. Fert, in *Ferromagnetic Materials*, edited by E. P. Wohlfarth (North-Holland, Amsterdam, 1982), Vol. 3, pp. 751–804.
[56] M. Kasami, T. Mishina, S. Yamamoto, and J. Nakahara, J. Lumin. **108**, 291 (2004).
[57] C. M. Varma, P. B. Littlewood, S. Schmitt-Rink, E. Abrahams, and A. E. Ruckenstein, Phys. Rev. Lett. **63**, 1996 (1989).
[58] M. A. Paalanen, J. E. Graebner, R. N. Bhatt, and S. Sachdev, Phys. Rev. Lett. **61**, 597 (1988).
[59] M. A. Paalanen, S. Sachdev, R. N. Bhatt, and A. E. Ruckenstein, Phys. Rev. Lett. **57**, 2061 (1986).
[60] M. P. Sarachik, A. Roy, M. Turner, M. Levy, D. He, L. L. Isaacs, and R. N. Bhatt, Phys. Rev. B **34**, 387 (1986).
[61] P. Coleman and C. Pepin, Phys. Rev. B **68**, 220405(R) (2003).
[62] P. Mehta, N. Andrei, P. Coleman, L. Borda, and G. Zarand, Phys. Rev. B **72**, 014430 (2005).
[63] A. Posazhennikova and P. Coleman, Phys. Rev. Lett. **94**, 036802 (2005).
[64] P. D. Sacramento and P. Schlottmann, J. Phys.: Condens. Matter **3**, 9687 (1991).